

SIMULATIONS AND OPTIMIZATIONS OF A NEW POWER COUPLER FOR 3.9-GHZ SUPERCONDUCTING CAVITIES AT FERMILAB*

Jianjian Li[†], Ivan Gonin, Timergali Khabiboulline, Daniel Olis, Nikolay Solyak[#],
FNAL, Batavia, IL 60510, U.S.A.

Thomas Wong, IIT, Chicago, IL 60616, U.S.A.

Abstract

3.9 GHz third harmonic superconducting cavities have been used to increase the peak bunch current and to compensate for non-linear distortions in the longitudinal phase space due to sinusoidal 1.3 GHz accelerating cavity voltage [1]. The power coupler is one of the important and complicated components of the third harmonic system for the TTF3 project. From electromagnetic, multipacting, and thermal simulations of the power coupler, optimized designs have been achieved, enabling one to minimize or eliminate potential problems in advance. This paper presents our recent work on simulation and optimization of the power coupler.

INTRODUCTION

The bunch length out of an RF gun is rather long (2mm in RMS) because of the strong 3D space charge coupling at low energy. The subsequent 1.3 GHz TESLA accelerating system will distort this long bunch in longitudinal phase space because of the induced cosine-like voltage curvature. A third harmonic system has been proposed to compensate for this kind of non-linear distortion and improve the peak bunch current. In the TTF3 project which is located at DESY in Germany a third harmonic system with four 3.9 GHz cavities will be installed after the first TESLA module, containing eight 1.3 GHz cavities, and before the first bunch compressor. The schematic layout of the injector is shown in figure 1.

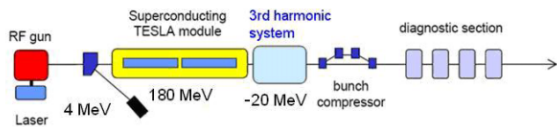


Figure 1: Schematic layout of TTF3 injector with the third harmonic system installed.

The total system (accelerating system and harmonic system) voltage up to second order is calculated [2] to be approximately constant within the bunch if the following conditions are met:

$$\phi_1 = -180^0, \text{ and} \tag{1}$$

$$V_1 = -\left(\frac{f_0}{f_1}\right)^2 \frac{V_0}{\cos(\phi_1)} \tag{2}$$

V_0 is the amplitude of the 1.3 GHz (f_0) RF system. V_1 is the amplitude of the harmonic RF system, which is

operated at the frequency f_1 with the relative phase ϕ_1 . Under the above conditions the sum of the two system voltages is:

$$V(s) \approx V_0 - V_1 = V_0 \left(1 - \left(\frac{f_0}{f_1}\right)^2\right) \tag{3}$$

From equations 2 and 3 we find that the frequency ratio determines the amplitude V_1 and total V .

We describe the design of the TTF3 3.9 GHz third harmonic system, the technology of which is required to support the new generation of linear colliders and high-quality free electron lasers.

POWER COUPLER DESIGN

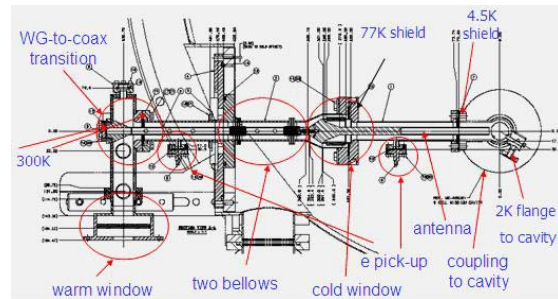


Figure 2: Fermilab developed 3.9 GHz power coupler.

Fermilab has developed a new 3.9 GHz power coupler [3] for the third harmonic cavities after a series of simulations and optimizations of different coupler designs. The final chosen layout of the power coupler shown in figure 2 is a 50 Ohm coaxial line with a 30mm diameter of outer conductor.

Table 1: Design Parameters of 3.9 GHz Power Coupler

Frequency	3.9 GHz
Pulse Length	1.3 ms (100us rise time)
Rep. Rate	5 Hz
Peak Power	45 kW for $I_{beam} = 9mA$ and $Q_{ext} = 9.5 \times 10^5$
Type	Coaxial
Window	Cylindrical and Planar (TiN coated)
Impedance	50 Ohm (6.5 mm/15 mm)
DC Biasing	No DC biasing due to multipacting-free design
Bellow Section	Two for mechanical flexibility
Cu Plated	All SS and Bellows
Waveguide	WG284
Coupling	Fixed (constant beam current)

*Work supported by U.S. Department of Energy

[†]lijianj@fnal.gov [#]solyak@fnal.gov

Detailed design parameters of the power coupler are shown in table 1. For the cold window, we adopted a cylindrical ceramic window coated with TiN to reduce the secondary yield coefficient. For the warm window, we used a waveguide planar window with good RF performance at operating frequency. We also applied a two-bellow-section design for obtaining better RF performance and more mechanical flexibility. A hollow antenna was used to reduce the mechanical stress on the cold window joint area. All components of the coupler were optimized for low power reflections at the operating frequency.

SIMULATION RESULTS

Electromagnetic Simulation

The system's external quality factor is a parameter, which needs to be set to couple the proper amount of power. The external quality factor of the cavity was calculated in equation 4 from a model shown in figure 3 with two couplers (in reality only half of geometry (4.5cells) was used with the electric boundary condition on the plane of symmetry).

$$Q_{ext_9cell} = 2 \times Q_{ext_calculated} \quad (4)$$

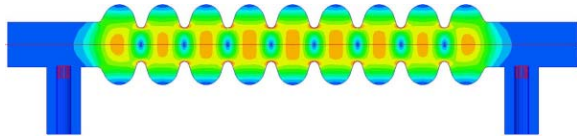


Figure 3: Electric field map of a nine-cell cavity model.

Generally the antenna may be inserted into the cavity tube to obtain higher coupling, as shown in figure 4 for the solid and hollow antennas. The hollow antenna provides an external quality factor within 4~6% higher than that of a solid antenna, independent of antenna penetration length.

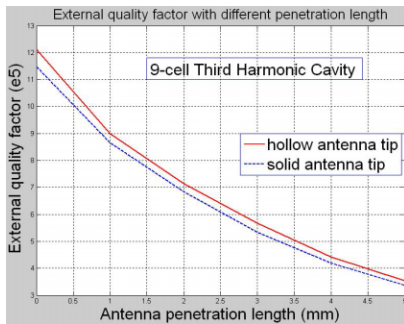


Figure 4: External quality factor for the nine-cell cavity with different antenna penetration length.

The power coupler has quite complicated geometry. Different parts of the coupler (cold window, bellow sections, coax-to-waveguide doorknob transition, pumping port, warm window) were optimized independently and then full geometry was simulated to check the resulting reflection coefficient. In figure 5, a series of reflection coefficients, S_{11} , for different coupler

components are shown. To define production tolerances we also studied the sensitivity of S_{11} to geometrical dimensions. After careful selection and optimization of the geometry and material, the reflection coefficients are kept very small.

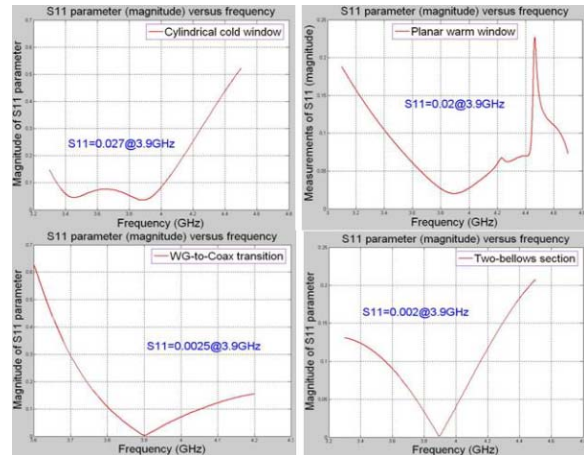


Figure 5: Reflection coefficients, S_{11} , for different coupler components.

Multipacting Calculation

Multipacting is a phenomenon of resonant electron multiplication in which a large number of electrons builds up an electron avalanche. This avalanche can abruptly absorb RF power and eventually lead to a breakdown.

For a coaxial line, both one-point multipacting (from outer conductor to itself) and two-point multipacting (from outer to inner conductor and back) may occur. The multipacting power for each case obeys quite accurately the following scaling laws [4]:

$$P_{one-point} \sim (f * d)^4 Z \quad (5)$$

$$P_{two-point} \sim (f * d)^4 Z^2 \quad (6)$$

where f is the RF operating frequency, d is the diameter of the outer conductor and Z is the line impedance. According to these scaling laws, we can select frequency and geometry parameters which optimize the multipacting power threshold. After optimization, we calculated several cases for our coaxial line including standing wave and traveling wave, and found the threshold of multipacting is about 420kW for traveling wave, which is substantially beyond our maximum operating power level. For standing wave, there is no electron multiplication if input power is less than 1MW.

Ceramic windows are usually made of alumina whose secondary yield coefficient can reach maximum values of 2 to 8. To reduce both surface charge buildup and the secondary yield coefficient, a thin Ti or TiN coating is generally deposited on its vacuum side. The secondary yield coefficient of Ti or TiN over a wide range of impact energies is less than unity, thus not leading to electron multiplication. Here we calculated three cases: mixed wave (partial reflection), standing wave (full reflection with electric or magnetic boundary) and traveling wave

(no reflection). We didn't find electron multiplication for standing wave and mixed wave if input power is below 1MW. For traveling wave, the threshold of multipacting is about 640kW, which is outside the range of our operating power levels.

Thermal Analysis

Thermally, the power coupler represents a connector from room temperature (300K) to the superconducting cryogenic environment (2K). At present the analysis includes two major heat transfer mechanisms: conduction and RF loss heating. Both static and dynamic regimes have been analyzed. Different copper plating thicknesses as well as different input powers were investigated in our model. 77K and 4.5K thermal intercepts were chosen to minimize the conduction and RF loss heating. Figure 6 shows the thermal analysis model built in ANSYS.

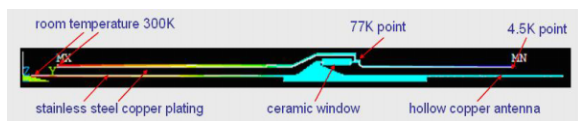


Figure 6: Thermal analysis model of the power coupler.

Temperature distributions along the surface of inner and outer conductors with different copper plating thicknesses and different input powers are shown in figure 7. We find the temperature distributions very sensitive to plating thickness [5]. If the plating is too thick, an additional static heat load is added to the thermal intercepts. If the plating is too thin, the electric field can penetrate into the stainless steel, causing more RF losses in the conductor. This will greatly increase the heat loads on the cryogenic system and the surface temperatures of the conductors. From figure 7 we also find most of the RF loss heating is imposed on the inner conductor, leading to a higher temperature increase.

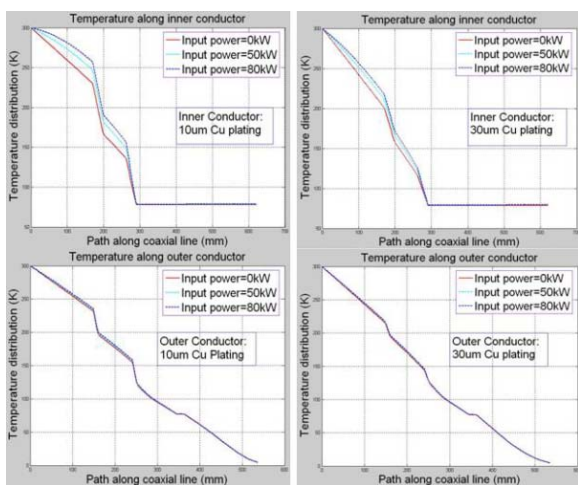


Figure 7: Temperature distributions along the surface of the inner and outer conductors for different plating thicknesses and input powers.

Calculated heat loads at the thermal intercepts of 77K and 4.5K points can be found in table 2. The heat loads at

4.5K point for 30um plating thickness are more than twice of that for 10um plating thickness. Finally we choose a 30um plating thickness for the inner conductor to obtain lower temperatures and a 15um plating thickness for the outer conductor to acquire smaller heat loads.

Table 2: Heat loads at 4.5K and 77K thermal intercepts.

Power & Plating Thickness	Ceramic Window (Max. T.)	4.5K Point	77K Point (from ceramic, from outer, total)
Unit: kW, um	K	W	W
0, 10	77.7	0.50	0.42+0.97=1.39
0, 30	78.4	1.15	0.78+1.04=1.82
50, 10	78.2	0.5	0.74+1.00=1.74
50, 30	78.8	1.16	1.13+1.04=2.17
80, 10	78.5	0.50	0.94+1.02=1.96
80, 30	79.1	1.16	1.34+1.08=2.42

CONCLUSION

From the simulation results, optimized designs have been obtained which can minimize potential problems in advance. The power couplers described in this paper will meet the strict requirements of the third harmonic system.

FUTURE PLAN

Six power couplers have been fabricated in industry and already delivered to Fermilab. After initial inspection and measurements, power couplers will be assembled on the coupler test stand for the high power RF testing and processing in the following several months.

REFERENCES

- [1] N. Solyak et al., "Development of the Third Harmonic SC Cavity at Fermilab," Proceedings of the 2003 Particle Accelerator Conference, Portland, Oregon, May 2003, p. 1213.
- [2] J. Sekutowicz et al., "A Design of a 3rd Harmonic Cavity for the TTF 2 Photoinjector," TESLA-FEL Report 2002-05.
- [3] D. Arnold et al., "Power Couplers Design for Third Harmonic and Spoke Cavities at Fermilab," Proceedings of the 12th Workshop on RF Superconductivity, Ithaca, New York, July 2005.
- [4] E. Somersalo, P. Yla-Oijala, and D. Proch, "Analysis of Multipacting in Coaxial Lines," Proceedings of the 1995 Particle Accelerator Conference, Dallas, Texas, May 1995, p. 1500.
- [5] M. Dohlus, D. Kostin, and W.D. Moller, "TESLA RF Power Coupler Thermal Calculations," Proceedings of the 2004 Linear Accelerator Conference, Lubeck, Germany, August 2004, p. 174.